very high brightnesses and efficiencies. The successful synthesis of these complexes provides a new direction for electrophosphorescent materials. Studies on the improvement of device structure, the design of new alkenylpyridine ligands, and the application of these ligands in the synthesis of cyclometallated heavy-metal complexes are currently underway.

## *Experimental*

*Procedure for Synthesizing $(PEP)_2Ir(acac)$*: PEP (2.2 mmol) was dissolved in 2-ethoxyethanol (10 mL) in a 50 mL round-bottom flask. Iridium trichloride hydrate (1.0 mmol) and water (3.0 mL) were then added to the flask. The mixture was stirred under nitrogen at 80 °C for 12 h. The mixture was cooled to room temperature and the precipitate was collected and washed with ethanol, followed by acetone, and then dried in vacuum to give the corresponding cyclometallated Ir(III)-$\mu$-chloro-bridged dimer. In a 50 mL flask, the dimer complex, acetylacetone (5.0 mmol) and $Na_2CO_3$ (10.0 mmol) were mixed with 2-ethoxyethanol (15 mL) and the mixture was refluxed at 80 °C under nitrogen for 12 h. After cooling to room temperature, 2-ethoxyethanol was distilled out. The residue was dissolved in dichloromethane and the solid was filtered off. The solution was concentrated in vacuo and the residue was purified on a silica gel column using a mixture of $CH_2Cl_2$ and hexane as eluent giving the desired iridium complex [Ir(PEP)$_2$(acac)]. The product was then sublimated at 200–220 °C and at a $4 \times 10^{-3}$ Pa prior to device fabrication. Similar procedures were also employed for the synthesis of other iridium complexes except Ir(PP)$_2$(acac). The Ir(PP)$_2$(acac) was synthesized in 72 % yield, using 3.0 equiv. of ligand (PP) for the initial step.

*$(PEP)_2$ Ir (acac):* $^1$H NMR ($CDCl_3$, 500 MHz) $\delta$ [ppm]: 1.81 (s, 6 H), 5.12 (s, 1 H), 6.56 (td, $J = 1.5$ Hz, $J = 6.0$ Hz, 2 H), 6.73 (s, 2 H), 6.90–6.92 (m, 10 H), 7.09 (d, $J = 7.5$ Hz, 2 H), 7.29 (td, $J = 1.5$ Hz, $J = 7.5$ Hz, 2 H), 7.78 (d, $J = 6.0$ Hz, 2 H). HRMS (EI) $m/z$ calcd. for $C_{31}H_{27}IrN_2O_2$ 652.1702; found 652.1699.

The devices were fabricated following the method reported previously [9].

Received: February 2, 2004
Final version: March 15, 2004
Published online: October 11, 2004

[1] a) *Organic Electroluminescent Materials and Devices*, (Eds: S. Miyata, H. S. Nalwa), Gordon and Breach Publishers, Amsterdam, The Netherlands **1997**, Chs. 5, 8, 12, 14. b) C. W. Tang, S. A. Van slyke, C. H. Chen, *J. Appl. Phys.* **1989**, *65*, 3610.

[2] a) R. F. Friend, R. W. Gymer, A. B. Holmes, J. H. Burroughes, R. N. Marks, C. Taliani, D. C. Bradley, D. A. Dos Santos, J. L. Bredas, M. Loglund, W. R. Salaneck, *Nature* **1999**, *397*, 121. b) A. J. Heeger, *Angew. Chem. Int. Ed.* **2001**, *40*, 2591.

[3] a) M. A. Baldo, D. F. O'Brien, Y. You, A. Shoustikov, S. Sibley, M. E. Thompson, S. R. Forrest, *Nature* **1998**, *395*, 151. b) M. A. Baldo, S. Lamansky, P. E. Burrows, M. E. Thompson, S. R. Forrest, *Appl. Phys. Lett.* **1999**, *75*, 4. c) D. F. O'Brien, M. A. Baldo, M. E. Thompson, S. R. Forrest, *Appl. Phys. Lett.* **1999**, *74*, 442.

[4] a) V. V. Grushin, N. Herron, D. D. LeCloux, W. J. Marshall, V. A. Petrov, Y. Wang, *Chem. Commun.* **2001**, 1494. b) H. Z. Xie, M. W. Liu, O. Y. Wang, X. H. Zhang, C. S. Lee, L. S. Hung, S. T. Lee, P. F. Teng, H. L. Kwong, H. Zheng, C. M. Che, *Adv. Mater.* **2001**, *13*, 1245.

[5] a) Y. Wang, N. Herron, V. V. Grushin, D. LeCloux, V. Petrov, *Appl. Phys. Lett.* **2001**, *79*, 449. b) J. P. J. Markham, S. C. Lo, S. W. Magennis, P. L. Burn, I. D. W. Samuel, *Appl. Phys. Lett.* **2002**, *80*, 2645. c) J. C. Ostrowski, M. R. Robinson, A. J. Heeger, G. C. Bazan, *Chem. Commun.* **2002**, 784.

[6] a) C. Adachi, M. A. Baldo, S. R. Forrest, M. E. Thompson, *Appl. Phys. Lett.* **2000**, *77*, 904. b) M. Ikai, S. Tokito, Y. Sakamoto, T. Suzuki, Y. Taga, *Appl. Phys. Lett.* **2001**, *79*, 156. c) C. Adachi, M. A. Baldo, M. E. Thompson, S. R. Forrest, *J. Appl. Phys.* **2001**, *90*, 5048.

[7] a) S. Lamansky, P. Djurovich, D. Murphy, F. Abdel-Razzaq, H. E. Lee, C. Adachi, P. E. Burrows, S. R. Forrest, M. E. Thompson, *J. Am. Chem. Soc.* **2001**, *123*, 4304. b) S. Lamansky, P. Djurovich, D. Murphy, F. Abdel-Razzaq, R. Kwang, I. Tsyba, M. Bortz, B. Mui, R. Bau, M. E. Thompson, *Inorg. Chem.* **2001**, *40*, 1704.

[8] a) A. B. Tamayo, B. D. Alleyne, P. Djurovich, S. Lamansky, I. Tsyba, N. N. Ho, R. Bau, M. E. Thompson, *J. Am. Chem. Soc.* **2003**, *125*, 7377. b) T. Akira, I. Hironobu, F. Manabu, M. Taihei, K. Jun, I. Satoshi, M. Takashi, M. Sieshi, T. Tahao, O. Shinjiro, H. Mikio, U. Kazunori, *J. Am. Chem. Soc.* **2003**, *125*, 12 971.

[9] J. P. Duan, P. P. Sun, C. H. Cheng, *Adv. Mater.* **2003**, *15*, 224.

[10] Ligand Yields: 2-[(*E*)-2-phenyl-1-ethenyl]pyridine **PEP** (75 %); 2-[(*E*)-2-naphthyl-1-ethenyl]pyridine **NEP** (72 %); 2-[(*E*)-2-phenyl-1-ethenyl]-5-(trifluoromethyl) pyridine **PETP** (72 %); 5-methyl-2-[(*E*)- 2-phenyl-1-ethenyl]pyridine **MPEP** (58 %); 2-[(*E*)-1-propenyl] pyridine, 2-[(*Z*)-1-propenyl]pyridine **PP** (63 %).

[11] a) J. W. Labadie, D. Tueting, J. K. Stille, *J. Org. Chem.* **1983**, *48*, 4634. b) M. F. Lappert, K. Jones, *J. Organomet. Chem.* **1965**, *3*, 295.

[12] C. W. Huang, M. Shanmugasundaram, H. M. Chang, C. H. Cheng, *Tetrahedron* **2003**, *59*, 3635.

[13] C. D. Poulter, M. Muehlbacher, D. R. Davis, *J. Am. Chem. Soc.* **1989**, *111*, 3740.

[14] A. K. Ghosh, C. Mukhopadhyay, U. R. Ghatak, *J. Chem. Soc., Perkin Trans. 1* **1994**, 327.

# Biodegradable Microfluidics**

By *Kevin R. King*, *Chiao Chun J. Wang*, *Mohammad R. Kaazempur-Mofrad*, *Joseph P. Vacanti*, and *Jeffrey T. Borenstein**

Biodegradable polymers are employed in many areas of therapeutic medicine, from commonly used resorbable surgical sutures[1] to next-generation controlled-release vehicles[2] and implantable cell-support scaffolds.[3] New applications in drug

[*] Dr. J. T. Borenstein, K. R. King,[+] C. C. J. Wang[++]
Charles Stark Draper Laboratory
Cambridge, MA 02139 (USA)
E-mail: jborenstein@draper.com
Dr. M. R. Kaazempur-Mofrad
Department of Mechanical Engineering
Massachusetts Institute of Technology
Cambridge, MA 02139 (USA)
Dr. J. P. Vacanti
Department of Surgery
Massachusetts General Hospital and
Harvard Medical School
Boston, MA 02114 (USA)
[+] Current address: Center for Engineering in Medicine
Massachusetts General Hospital and Harvard Medical School,
Boston, MA 02114, USA.
[++] Current address: Department of Biomedical Engineering,
Johns Hopkins University Baltimore, MD 21205, USA.

[**] This project was sponsored by the Department of the Army, Cooperative Agreement DAMD-99-2-9001. The content of this paper does not necessarily reflect the position or the policy of the government, and no official endorsement should be inferred.


DOI: 10.1002/adma.200306522

ADVANCED MATERIALS

delivery and tissue engineering are demanding improved design flexibility and microscale control in order to localize small volumes of potent therapeutic agents,[4] control drug-release kinetics,[5] and construct optimized scaffolding for supporting and guiding the development of highly structured tissue.[6] Conventional biodegradable-polymer processing techniques such as solvent casting/porogen leaching,[7] gas foaming,[8] and fiber bonding[9] are limited to controlling bulk properties such as average pore size and porosity rather than individual pore size, shape, arrangement, and interconnectivity.[10] Recently, three-dimensional printing and solid free-form fabrication have dramatically improved design flexibility. However, spatial resolution is still limited to hundreds of micrometers[11] and vacuum-assisted removal of cytotoxic residual solvents still limits processing times to hours or days.[12] To date, no single technique has clearly demonstrated control of the broad range of required size scales (micrometers to centimeters)[6] with the necessary resolution, speed, and flexibility.

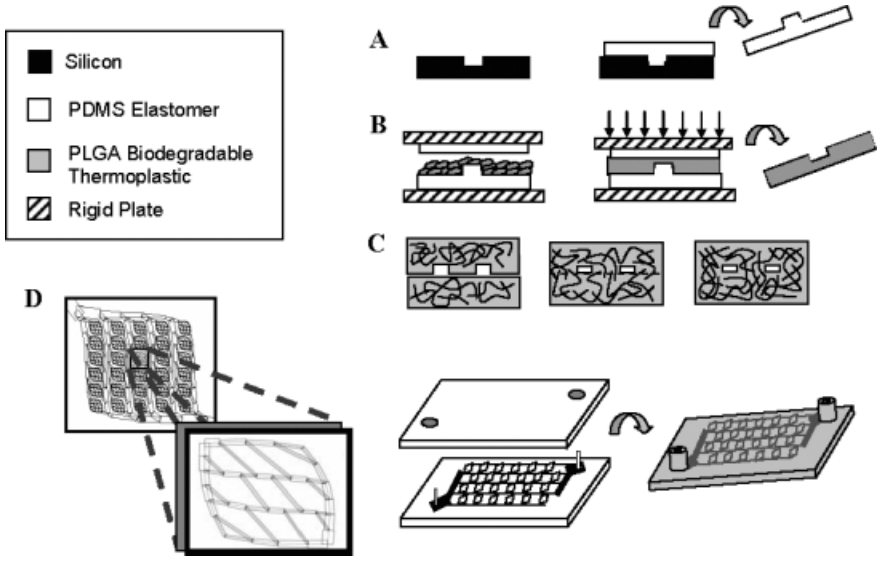


**Figure 1.** Overview of biodegradable microdevice fabrication. A) Photolithography is performed on a polished silicon wafer and used to create an inverse PDMS replica. B) Biodegradable PLGA 85:15 thermoplastic pellets are placed on the PDMS inverse mold, heated to a melt, and pressed with constant force between two rigid, metal plates. When cooled, the stack disassembled and a microstructured PLGA 85:15 film resulted. C) The microstructured PLGA 85:15 films consisted of high-molecular-weight linear-chain polymers. Using a pure thermal bonding process, the microstructured films achieved intimate contact, the polymer chains were mobilized, and bond strength developed through polymer-chain interdiffusion. After bonding, a monolithic, three-dimensional, biodegradable microdevice resulted. D) Complex microfluidic networks were designed using the MATLAB software, translated to photomasks, and used to create biodegradable PLGA 85:15 microfluidics. Inlets and outlets were formed by extruding PLGA melt through a two-part PDMS annular mold. A schematic of the PLGA microfluidic molding process with integrated inlets and outlets is shown.

Microfabrication is an excellent tool for controlling features at the size scale of individual cells and molecules.[13] However, adapting photolithographic processes to biodegradable polymers has not proven to be straightforward, in part because conventional biodegradable-polymer processing requires precipitation of films from dilute polymer solutions. Such solvent-based approaches were recently combined with microfabrication techniques, but solvent effects such as bubbles and drying-induced shrinkage still limit resolution and total device area.[14] Microfabrication presents an additional obstacle—it is fundamentally a two-dimensional technique. Delivery of therapeutically viable numbers of living cells, as is needed for engineering vital tissues, will require large three-dimensional devices that can maintain the spatial resolution, precision, and reproducibility to reliably interact with cells at small size-scales without compromising the capacity for scaling up.[15] Therefore, if photolithographic planar processing is to be effective as a scaffold fabrication technique, it must be complemented with a lamination strategy.

We have developed a scalable fabrication platform for constructing high-resolution, high-precision features in three-dimensional devices made entirely from the commonly used, prototypical, biodegradable thermoplastic, poly(DL-lactic-*co*-glycolide) 85:15 (PLGA 85:15) (Fig. 1). By melt-processing, we avoided the limitations associated with solvent-based processing and demonstrated fabrication of micrometer-scale features in biodegradable films. In addition, we also overcame the two-dimensional constraint of planar processing by stacking, aligning, and sealing interconnected, micropatterned films using a newly optimized thermal fusion bonding process. This general fabrication process for constructing monolithic, three-dimensional, biodegradable devices offers a unique strategy for building novel, implantable, drug-delivery devices, and complex tissue-engineering scaffolds with new functionality and improved performance. We demonstrate this potential here by constructing highly branched, multilayer PLGA microfluidic networks, analogous to tissue microvasculature, for large-scale tissue engineering.

Figure 1 illustrates the microfabrication process. High-resolution microstructured master molds were first created using conventional photolithography and silicon micromachining (Fig. 1A).[16] A poly(dimethylsiloxane) (PDMS) silicone elastomer was then cast, cured, and peeled from the silicon master to create non-adhesive flexible tooling for subsequent PLGA-melt molding. Biodegradable PLGA pellets were heated to a melt on the PDMS tooling and pressed with constant force between two flat, rigid, parallel plates to create thin, microstructured, PLGA films (Fig. 1B). The film thicknesses (100–500 μm) were controlled by varying the compression time (2–15 min), temperature (110–150 °C), and applied force (100–500 lbs; 1 lb ≈ 0.45 kg), guided by the Stefan equation for radial flow of a temperature-dependent viscous fluid between parallel plates.[17] Once compressed, the stack was

  

cooled to below the PLGA glass-transition temperature ($T_g = 50\,°C$, as determined by differential scanning calorimetry),[18] and the flexible PDMS tooling was peeled from the newly microstructured PLGA. To determine the extent of thermal degradation caused by the melt molding, we performed thermal gravimetric analysis under nominal fabrication-process conditions and found the rate of mass loss to be less than 0.01 % $min^{-1}$.[19]

Scanning electron micrographs of microstructured PLGA films are shown in Figure 2. The high-fidelity transfer of the complex microfluidic channel network design shown in Figure 1D clearly demonstrates that, despite the elastic nature of the PDMS tooling, the molded PLGA channels exhibit sharp corners; this is important for subsequent bonding (Fig. 2A).

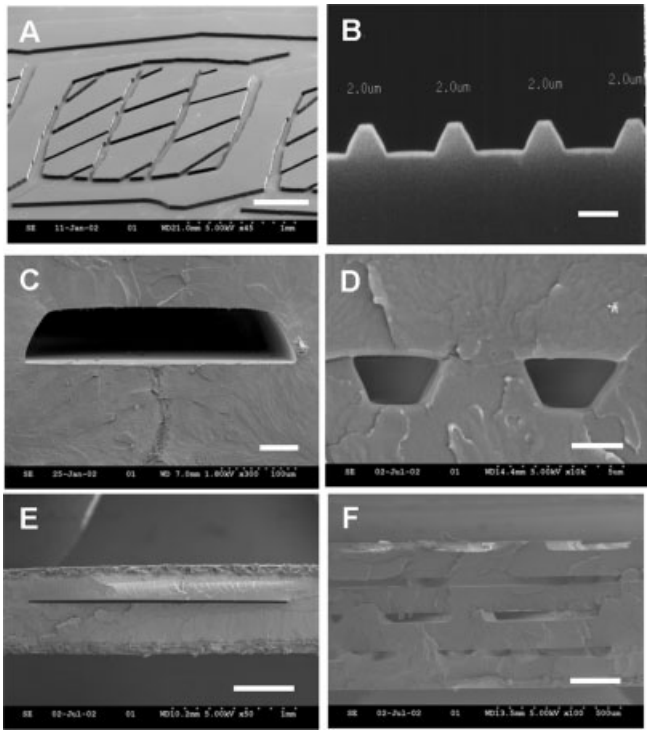


**Figure 2.** Electron micrographs of biodegradable precision microstructures: A) complex branching network of microchannels (scale bar: 500 ▫m); B) high-resolution lines (scale bar: 2 ▫m); C) nominal microfluidic channel cross-section (scale bar: 50 ▫m); d) high-resolution microchannels (scale bar: 2 ▫m); E) fully bonded high-aspect-ratio (width/height ratio 200:1) microchannel (scale bar: 500 ▫m); and F) multilayer microfluidic networks—four layers bonded in a single thermal bonding step (scale bar: 200 ▫m).

Furthermore, because the PLGA films were molded from PDMS tooling originally cast on polished silicon, the bonding surfaces were exceptionally flat and were reliably stacked, aligned, and fusion bonded. The formation of 2 ▫m wide channels (Fig. 2B) demonstrate that PLGA micromolding can be performed at the resolution limit of the photolithography process, offering exceptional reproducibility (~0.1 ▫m precision) and enabling definition of PLGA structures with subcellular spatial resolution.

After patterning, the PLGA microstructured films must be laminated to form fully biodegradable, three-dimensional structures. Previous approaches to bonding biodegradable polymers have required the use of non-biodegradable intermediate adhesion layers[18] or employed solvent welding,[20] which tends to distort surface microstructures. More recently, solvent-cast, microstructured films were laminated with the assistance of temperature manipulation.[14] In contrast to previous studies, we have developed a purely thermal fusion bonding process that works in the complete absence of solvents. Heating aligned films modestly above the PLGA glass-transition temperature mobilized high-molecular-weight polymer chains and allowed interdiffusion across the macroscopic bond interface[21] accompanied by the development of an associated interfacial bond strength (Fig. 1C).[22,23] As interdiffusion proceeded, cross-section inspections revealed a monolithic structure with complete disappearance of the bond interface. Figure 2C shows a cross-section of a nominal microchannel with no observable bond interface and no thermally induced channel deformation. As further evidence that fusion bonding was sufficiently complete, constructs subjected to destructive peel tests were found to break in the bulk before breaking at the interface, indicating that the interfacial strength was comparable to the cohesive strength of the material.[24] We have used this process to fabricate a wide range of closed microstructures with channel widths ranging from micrometers to millimeters. Figure 2D demonstrates a resulting high-resolution monolithic microchannel that might find use as a size-selective conduit, constraining cell migration while allowing chemical communication via diffusible soluble mediators.

Careful control of time and temperature are critical to the thermal fusion bonding of microstructures because the elastic modulus of thermoplastics is highly temperature dependent near the glass-transition temperature.[25] If the bonding temperature is too high or the bonding time too long, the thin viscoelastic microchannel ceilings would deform and collapse under their own weight. However, at the other extreme, interdiffusion can be so slow that the time required to achieve sufficient bond strength is prohibitively long (>24 h). Therefore, we developed a first-order model of these processes and identified a "process window" (the difference between the "time to deformation" and the "interdiffusion bonding time") by characterizing the temperature dependence of the elastic modulus and modeling the collapsing microchannel ceilings as thin, temperature-sensitive, viscoelastic beams falling under their own weight. Using the model, deformation times were successfully predicted as functions of channel height, channel width, film thickness, and bonding temperature. This thus allowed the process conditions to be optimized for specific device geometries (manuscript in preparation). Aided by the model, we have shown that even the most challenging channels—the wide, shallow channels (Fig. 2E; width to depth ratio of 200 )—can be bonded without appreciable plastic deformation. Thermal fusion bonding is also particularly well-suited to the fabrication of three-dimensional structures be-

  

ADVANCED MATERIALS

cause many films can be bonded simultaneously in a single heating cycle (Fig. 2F). As an example of typical process parameters, microchannels with 50 μm heights would be bonded for 10–60 min at 65–75 °C, depending on the exact film thickness and the maximum microchannel width.

Functional microfluidic networks were created by combining melt micromolding and fusion bonding with an extruded inlet–outlet scheme. First, vertical elastomeric posts were bonded to the PDMS tooling at the location of the inlet and outlet. Next, larger holes were punched in a second ~1 cm thick unpatterned PDMS film aligned to the vertical posts. When the PLGA melt was compressed between the two PDMS molds, the viscous polymer was vertically extruded and annular PLGA inlets and outlets were formed (Fig. 1D). These films were then readily bonded to other planar layers to form fully patent, biodegradable, microfluidic networks. Figure 3A shows a large 3 cm × 3 cm hierarchical, microfluidic network with widths ranging from 30 μm to 3000 μm and with universal channel heights of 35 μm. When perfused, the networks showed no signs of leaks, occlusions, or channel-to-channel cross-talk. Multilayer networks were enabled by fabricating tall, vertical posts in the otherwise unpatterned, top PDMS mold, where layer-to-layer communication was desired. When these PDMS posts contacted the bottom PDMS mold, they created through-holes or "vias" during PLGA-melt molding. Alignment of the PDMS molds was performed manually. Figure 3B shows a close-up of a fully perfused, three-dimensional device with multiple, interconnected, microfluidic layers.

A typical pressure-flow measurement from a single layer network is shown in Figure 3C. Theoretical fluidic resistances can be predicted by solving for the equivalent resistance of each straight segment by using the rectangular-duct solution to the viscous-dominated Navier–Stokes equation.[26] The resulting discrete resistor network can then be solved to predict the total fluidic resistance using commercial circuit-analysis software (PSPICE). The fabricated biodegradable networks were found to have linear pressure-flow characteristics that were in close agreement with theoretical fluidic resistances, demonstrating that the channels had negligible capacitance, and that the fluidic ducts were accurately fabricated to meet the functional and geometrical specifications. This confirmed the fidelity of the fabrication process and suggested that a wide range of devices can be rationalized mathematically prior to fabrication and can be constructed to meet specified design criteria.

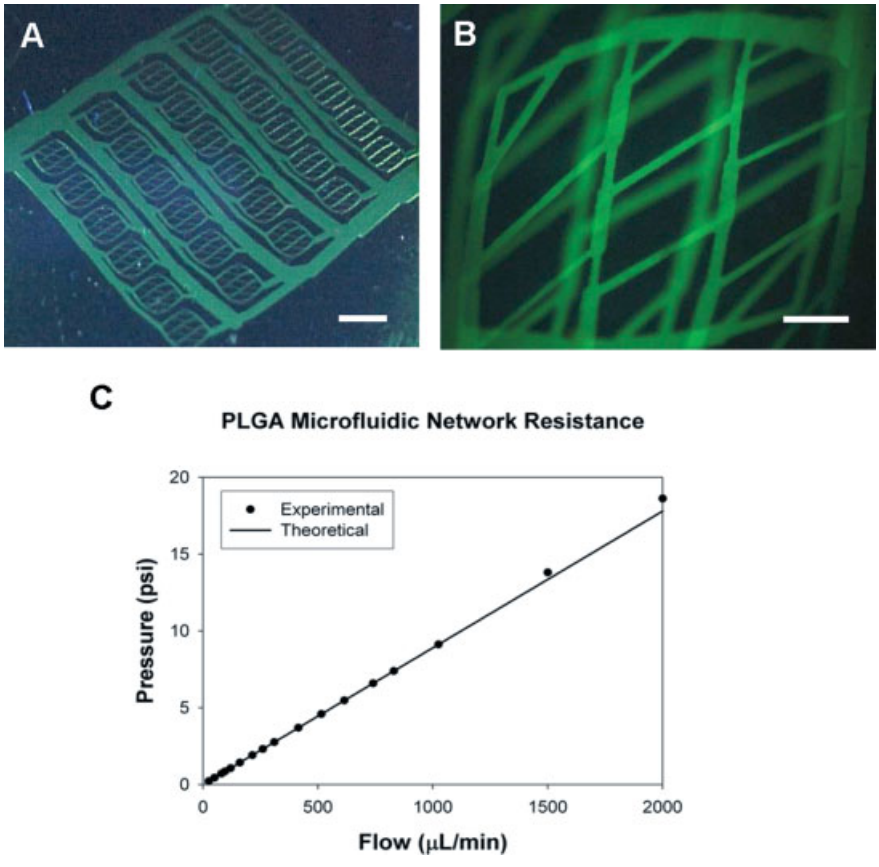


**Figure 3.** PLGA microfluidic networks were found to be readily perfused without leaks, occlusions, or interchannel cross-talk over a large-area device (~9 $cm^2$). A) Macroscopic image of a complete microfluidic network (scale bar: ~2.5 mm), B) Close-up of a multilayer network perfused with fluorescein dye (scale bar: ~300 μm). C) Experimental pressure–flow relationships (compared to theoretical) for the PLGA microfluidic network.

The fabrication platform described here combines precision, speed, and scalability to build high-performance, biodegradable microdevices. Once microfabricated masters are created, elastomeric and thermoplastic replicas can be rapidly and repeatedly generated without expensive equipment. The shift from solvent-based processing to melt micromolding is a key advantage of this approach. Solventless approaches allow exquisite geometrical control and reproducibility that are not possible using solvent casting. Furthermore, the resulting microchannels have predictable mechanical strength and can withstand thermal fusion bonding without deformation or collapse, lending the approach three-dimensionality and scalability.

Ultimately, we envision that this platform can be extended to achieve exciting new functionality by incorporating many recent developments in the fields of microfluidics, tissue engineering, and drug delivery. For example, well-established cell-patterning techniques can be employed to arrange multiple cell types and organize complex tissue architecture. To demonstrate the feasibility of seeding and culturing cells in microscale

  

geometries, we have recently performed long-term, continuous-flow endothelialization of prototype elastomeric microfluidic networks (manuscript in preparation). Since the newly developed thermal fusion bonding requires relatively low bonding temperatures, it might be possible to incorporate biologically active macromolecules into the constructs to facilitate coordinated tissue growth. As a first step, we have recently demonstrated that commonly used PLGA microspheres and porous scaffolds, fabricated using traditional techniques, can be readily fusion-bonded to the microstructured films (data not shown), making this fabrication approach complementary to conventional techniques rather than an alternative. Finally, the micromolding strategy is generalizable and suitable for adaptation to new, biodegradable polymers such as high-functionality, shape-memory, degradable materials[27] and the recently developed elastomeric "biorubber."[28]

Biodegradable cell-support scaffolds play a critical role in the growth of engineered tissue and the delivery of biologically active agents. However, most scaffolds rely solely on diffusive transport and are therefore limited to being on a millimeter size-scale. The microfluidics described here offer an opportunity to complement diffusion with convective transport. In the same way that blood-carrying capillaries reduce the tissue diffusive distances to ~100 μm in vivo, integrated, biodegradable, microfluidic channels can reduce diffusion distances in cell-seeded scaffolds and allow them to be scaled up considerably.

Surmounting the challenges of tissue engineering will ultimately require methods for guiding rapid vascularization, recapitulating normal tissue architecture, coordinating the orchestrated release of multiple active macromolecules, and scaling-up scaffolds to deliver therapeutically viable numbers of highly functional parenchymal cells. The techniques described in this paper offer a flexible fabrication platform for creating such devices, using a rational scaffold design. A priori calculation of structural parameters such as total surface area and surface-area-to-volume ratios, as well as functional parameters such as metabolite transport and cell-surface shear stress, will allow rapid optimization of cell attachment and growth. In the area of drug delivery, microscale cavities, capsules, and microchannels can be designed to control the release location, species, and kinetics to modify the complex biomolecular environment with spatiotemporal specificity. Using the new biodegradable microfabrication process, tissue engineers and drug delivery developers can more systematically vary critical scaffold properties, and efficiently explore the large parameter space linking scaffold geometry and controlled release to tissue development.

We have described a significant advancement in biodegradable polymer processing—a rapid, versatile, and low-cost approach to precision building biodegradable microdevices from microstructured PDMS molds. Stacking and bonding micropatterned films with a parallel thermal fusion bonding process enabled rapid fabrication of three-dimensional monolithic microdevices containing a wide range of surface microstructures. We have demonstrated this technology by constructing robust, multilayer, microfluidic networks with extruded inlets and outlets, and shown that they can be reliably perfused without leaks or occlusions. Compared to previous methods, this fabrication approach represents more than an order of magnitude improvement in speed, resolution, and precision, while providing unmatched reproducibility, manufacturability, and scalability, thus making it ideal for large-scale engineering of complex tissues and high-performance, biodegradable, medical devices.

## *Experimental*

*Silicon Master and Elastomeric Tooling Fabrication*: Standard cleanroom photolithography was used to fabricate features on or in silicon wafers using combinations of thick SU-8 photosensitive epoxy (SU-8 Clariant), anisotropic bulk silicon etching (STS), or thin-film positive photoresist (AZ 5214 Clariant) to achieve a variety of feature thicknesses and cross-sectional geometries. The PDMS silicone elastomer (Sylgard 184 Dow Corning) prepolymer was prepared by mixing 10:1 resin/curing agent, degassing under vacuum, casting on the microstructured silicon mold, curing at 80 °C for 3 h, and peeling the flexible and durable inverse mold for use as tooling in subsequent melt micromolding processes.

*Biodegradable Micromolding*: The PDMS mold was placed on a preheated (110 °C–150 °C) leveled hotplate, and the microstructured PDMS surface (~1–20 $cm^2$) was covered with PLGA 85:15 polymer pellets (~2 mm thick; Medisorb, Alkermes). A second PDMS film (patterned or unpatterned) was placed on the pellets for several minutes, allowing the pellets to soften and form a highly viscous melt. A rigid plate was then placed on the unpatterned PDMS film and a compressive force (100–500 lbs; 1 lb ≈ 0.45 kg) was applied perpendicular to the stack for 5–15 min using a press such as an Instron mechanical tester or a large c-clamp. After reaching room temperature, the stack was cooled and disassembled, and the microstructured PDMS tooling was then ready for molding the next layer. We have reused the microfabricated PDMS tooling upwards of 30 molding cycles without breaking. Once the reusable PDMS molds were fabricated, each microstructured, biodegradable film required only 5–15 min to fabricate. Time, temperature, force, and sample size were used to control the thickness, guided by the Stefan equation for radial-squeeze flow between parallel plates under constant compressive force [17]. Typical resulting film thicknesses were between 100 μm and 500 μm.

*Thermal Fusion Bonding*: Three-dimensionality was achieved by stacking and bonding microstructured PLGA films in a large convection oven. The substrates were aligned manually under a microscope and bonded isothermally in a convection oven between 60 °C and 80 °C, depending on the microstructure geometries (65–75 °C was optimal for most devices). Bonding times ranged from 20–120 min depending on the temperature. Bonding could have been monitored by gross or microscopic examination of the samples. When the two surfaces initially achieved intimate contact or "wet", a distinct color change was observable. Once the samples reached the bonding temperature, moderate, diffuse, finger pressure could have been applied to assist intimate contact if it was incomplete.

*Biodegradable Microfluidics*: A complex microfluidic network with hierarchical branching patterns and small channel interconnections on the same size scale as physiologic capillaries was designed. The grossly parallel design was intended to allow continuous-flow delivery of soluble metabolites to seeded cells without exposing them to phenotype-altering shear stress.

*Extruded Fluidic Connections*: An extruded fluidic connection scheme was implemented to allow "macroworld" fluidic access to the microfluidic networks using standard silastic tubing (Du Pont). The scheme involved modification of the PDMS inverse mold. Drilling a

  

ADVANCED MATERIALS

thick slab of PDMS with a blunted and beveled syringe needle created small-diameter PDMS posts, which were bonded to the micropatterned PDMS layer at the location of the microfluidic network inlet and outlet, using a small drop of PDMS prepolymer. In a second unpatterned layer of PDMS, large diameter holes (7 mm) were punched, spaced to overlay the inlet and outlet of the network. When the two layers were mated, they defined an annular structure through which the PLGA melt could be extruded during the compression micromolding process. This allowed fabrication of robust, vertical, biodegradable posts that could be fit with flexible tubing for perfusion.

*Perfusion*: Silastic tubing was secured with epoxy. Networks could be repeatedly pressurized above 50 psi (1 psi ~ 0.0703 kg cm$^{-2}$) without breaking, an order of magnitude larger than the pressures experienced in vivo by physiological blood vessels. The fluidic resistance was readily characterized experimentally using a constant-flow syringe pump (Harvard PHD 2000) and a digital pressure sensor (Meritech), and it was found to match theoretical predictions within experimental error. For theoretical predictions, each straight, channel segment was treated as a discrete, fluidic resistor with a constant rectangular cross-section (Fig. 3C). The rectangular-duct solution to the Navier–Stokes equation allowed calculation of segment resistances and the resulting discrete resistive network was solved using the PSPICE circuit simulator. Multilayer networks involved either micromolded through-holes or punched vertical "vias" at the inlet and outlet, and all networks were perfused with an aqueous fluorescein salt solution (Sigma).

Received: November 25, 2003
Final version: July 13, 2004

[1] R. P. Lanza, R. Langer, W. L. Chick, in *Principles of Tissue Engineering* (Eds: R. P. Lanza, R. Langer, W. L. Chick), Academic Press, Austin, TX **1997**.
[2] D. A. La Van, D. M. Lynn, R. Langer, *Nat. Rev. Drug Discovery* **2002**, *1*, 77.
[3] J. P. Vacanti, R. Langer, *Lancet* **1999**, *354 (Suppl. I)*, 32SI.
[4] J. T. Santini, M. J. Cima, R. Langer, *Nature* **1999**, *397*, 335.
[5] L. Leoni, T. Boiarski, T. A. Desai, *Biomed. Microdevices* **2002**, *4*, 131.
[6] S. N. Bhatia, C. S. Chen, *Biomed. Microdevices* **1999**, *2*, 131.
[7] W. L. Murphy, R. G. Dennis, J. L. Kileny, D. J. Mooney, *Tissue Eng.* **2002**, *8*, 43.
[8] L. D. Harris, B.-S. Kim, D. J. Mooney, *J. Biomed. Mater. Res.* **1998**, *42*, 396.
[9] A. G. Mikos, Y. Bao, L. G. Cima, D. E. Ingber, J. P. Vacanti, R. Langer, *J. Biomed. Mater. Res.* **1993**, *27*, 183.
[10] S. Yang, K.-F. Leong, Z. Du, C.-K. Chua, *Tissue Eng.* **2001**, *7*, 679.
[11] S. Yang, K.-F. Leong, Z. Du, C.-K. Chua, *Tissue Eng.* **2002**, *8*, 1.
[12] W. S. Koegler, C. Patrick, M. J. Cima, L. G. Griffith, *J. Biomed. Mater. Res.* **2002**, *63*, 567.
[13] G. M. Whitesides, E. Ostuni, S. Takayama, X. Jiang, D. E. Ingber, *Annu. Rev. Biomed. Eng.* **2001**, *3*, 335.
[14] G. Vozzi, C. Flaim, A. Ahluwalia, S. N. Bhatia, *Biomaterials* **2003**, *24*, 2533.
[15] J. T. Borenstein, H. Terai, K. R. King, E. J. Weinberg, M. R. Kaazempur-Mofrad, J. P. Vacanti, *Biomed. Microdevices* **2002**, *4*, 167.
[16] D. C. Duffy, J. C. McDonald, O. J. A. Schueller, G. M. Whitesides, *Anal. Chem.* **1998**, *70*, 4974.
[17] M. M. Denn, *Process Fluid Mechanics*, Prentice Hall, Englewood Cliffs, NJ **1980**.
[18] E. A. Turi, *Thermal Characterization of Polymeric Materials*, 2nd ed., Vol. 2, Academic Press, San Diego, CA **1997**.
[19] D. K. Armani, C. Liu, *J. Micromech. Microeng.* **2000**, *10*, 80.
[20] A. G. Mikos, G. Sarakinos, S. M. Leite, J. P. Vacanti, R. Langer, *Biomaterials* **1993**, *14*, 323.
[21] Y. H. Kim, R. P. Wool, *Macromolecules* **1983**, *16*, 1115.
[22] K. Aradian, E. Raphael, P.-G. de Gennes, *Macromolecules* **2000**, *33*, 9444.
[23] R. P. Wool, K. M. O'Conner, *J. Appl. Phys.* **1981**, *52*, 5953.
[24] R. P. Wool, *Polymer Interfaces: Structure and Strength*, Hanser Gardner Publications, New York **1995**.
[25] A. S. Wineman, K. R. Rajagopal, *Mechanical Response of Polymers: An Introduction*, Cambridge University Press, Cambridge, UK **2000**.
[26] N.-T. Nguyen, S. T. Wereley, *Fundamentals and Applications of Microfluidics*, Artech House, Norwood, MA **2002**.
[27] Y. Wang, G. A. Ameer, B. J. Sheppard, R. Langer, *Nat. Biotechnol.* **2002**, *20*, 602.
[28] A. Lendlein, R. Langer, *Science* **2002**, *296*, 1673.

# Self-Assembly of the Mesoporous Electrode Material $Li_3Fe_2(PO_4)_3$ Using a Cationic Surfactant as the Template**

By *Shenmin Zhu*, *Haoshen Zhou*,* *Toshikazu Miyoshi*, *Mitsuhiro Hibino*, *Itaru Honma*, and *Masaki Ichihara*

The utilization of supermolecular assemblies of surfactant molecules as structure-directing templates has become a powerful and well-established method for the synthesis of ordered mesostructured materials.[1–6] This method has now been extended to the preparation of a mesoporous metal phosphate.[7–11] Materials containing a phosphate moiety are likely be attractive as new cathode materials.[7–13] Alternative cathode materials for lithium batteries, such as iron phosphates, are of particular importance because of their natural abundance and non-toxic nature. They are beginning to replace $LiCoO_2$, which is expensive and potentially poses an environmental risk.[14] $Li_3Fe_2(PO_4)_3$, which was first discov-

[*] Dr. H. Zhou, Dr. S. Zhu, Dr. M. Hibino, Dr. I. Honma
Energy Electronics Institute
National Institute of Advanced Industrial Science and Technology (AIST)
AIST Tsukuba Central
1-1-1 Umezono, Tsukuba, Ibaraki 305-8568 (Japan)
E-mail: hs.zhou@aist.go.jp
Dr. T. Miyoshi
Research Center of Macromolecular Technology
National Institute of Advanced Industrial Science and Technology (AIST)
AIST Tsukuba Central
1-1-1 Higashi, Tsukuba, Ibaraki 305-8565 (Japan)
Dr. M. Ichihara
Material Design and Characterization Laboratory
Institute for Solid State Physics
University of Tokyo
5-1-5 Kashiwanoha, Kashiwa, Chiba 277-8581 (Japan)

[**] S. Zhu acknowledges the financial support of the Japanese Society of the Promotion of Science Fellowship (JSPS) for work carried out at the Energy Electronics Institute, AIST, and thanks Y. Toda for help with TEM observations. H. Zhou is grateful for partial research funding from JSPS, AIST, JST, and the nanotechnology-supporting program of the Ministry of Education and Science, Japan. Supporting Information is available online from WileyInterScience, or from the author.

  DOI: 10.1002/adma.200400207 